High Temperature Air-Cooled Power Electronics Thermal Design

Annual Progress Report

Scot Waye

NREL is a national laboratory of the U.S. Department of Energy
Office of Energy Efficiency & Renewable Energy
Operated by the Alliance for Sustainable Energy, LLC

This report is available at no cost from the National Renewable Energy Laboratory (NREL) at www.nrel.gov/publications.

Management Report
NREL/MP-5400-62784
August 2016

Contract No. DE-AC36-08GO28308

NREL
NATIONAL RENEWABLE ENERGY LABORATORY

High Temperature Air-Cooled Power Electronics Thermal Design

Annual Progress Report

Scot Waye

Prepared under Task No. VTP2.7000

NREL is a national laboratory of the U.S. Department of Energy
Office of Energy Efficiency & Renewable Energy
Operated by the Alliance for Sustainable Energy, LLC

This report is available at no cost from the National Renewable Energy Laboratory (NREL) at www.nrel.gov/publications.

National Renewable Energy Laboratory
15013 Denver West Parkway
Golden, CO 80401
303-275-3000 • www.nrel.gov

Management Report
NREL/MP-5400-62784
August 2016

Contract No. DE-AC36-08GO28308

Cover Photos by Dennis Schroeder: (left to right) NREL 26173, NREL 18302, NREL 19758, NREL 29642, NREL 19795.

NREL prints on paper that contains recycled content.

High-Temperature Air-Cooled Power Electronics Thermal Design

Susan Rogers (APEEM Technology Development Manager)
Subcontractor: National Renewable Energy Laboratory (NREL)

Sreekant Narumanchi (NREL Task Leader)
Scot Waye (Principal Investigator)
National Renewable Energy Laboratory
15013 Denver West Parkway
Golden, CO 80401
Phone: (303) 275-4062
E-mail: sreekant.narumanchi@nrel.gov

Start Date: FY11
Projected End Date: FY14

Objectives

The overall project objective is to develop and apply air-cooling technology to improve power electronics thermal management design and influence industry, enhancing system performance to help meet the U.S. Department of Energy (DOE) Advanced Power Electronics and Electric Motors (APEEM) Program power electronics technical targets for weight, volume, cost, and reliability. This overall objective includes the following:

- Develop and demonstrate commercially viable, low-cost air-cooling solutions for a range of vehicle applications and assess their potential for reducing the cost and complexity of the power electronics cooling system
- Enable heat rejection directly to ambient air, simplifying the system by eliminating liquid coolant loops, thereby improving weight, volume, cost, and reliability
- Collaborate with Oak Ridge National Laboratory (ORNL) to demonstrate the feasibility of using a high-temperature, air-cooled inverter to achieve DOE technical targets
- FY 14 objectives included:
  - Prototype and test optimized heat exchanger. Improve models based on test results. Down select best design for prototype module
  - Test baseline and optimized heat exchangers. Extrapolate results to inverter level, including balance-of-inverter components and balance-of-system metrics
  - Within electrical topology constraints, test module-level heat exchanger design for thermal performance. Results will feed into improved design and future high-temperature, air-cooled inverter demonstration with ORNL.

Technical Barriers

The use of air as a coolant has several benefits, drawbacks, and challenges. Air is free, it does not need to be carried, it is benign (no safety or environmental concerns), and it is a dielectric. As a heat transfer fluid, however, it has a number of drawbacks. Air has a low specific heat, low density, and low conductivity. These make it a poor heat transfer fluid and cause a number of design challenges. To reject the high power densities required by electric-drive power electronics using the heat transfer coefficients achievable with air, large increases in wetted area are needed. When increasing the wetted area, spreading resistance, fin efficiency, weight, volume, and cost need to be considered. Due to the low specific heat, larger mass flows of air are required to remove the heat. This can lead to parasitic power issues, especially coupled to the pressure loss of extended surfaces. This requires careful consideration of the system coefficient of performance. Depending on the location of the inverter, environmental loads and ducting to better air sources may need to be considered. Location can also affect the need for noise suppression for the prime mover (blower/fan). For example, the Honda system incorporated a silencer [1] because the inverter was located in the passenger compartment. To push heat transfer performance higher, small-channel heat exchangers can be used, but filtering must be addressed. If needed, filtering can add pressure drops and maintenance issues may need to be addressed.

Technical Targets

The 2015 and 2020 DOE APEEM Program technical targets for power electronics are applicable for a 30-kW continuous and 55-kW peak power inverter.

Accomplishments

- Shifted modeling efforts that optimized heat exchanger geometries to experimental efforts
- Tested baseline and optimized sub-module heat exchangers for maximum junction temperatures of 150°C to 300°C
- Extrapolated results to inverter scale
- Target heat load of 2.7 kW was dissipated at various flow rates for each of the configurations
- Combining optimized heat exchanger with other inverter components (excluding housing), estimated power density and specific power exceeded 2015 technical targets
- Module-level heat exchanger tested with one-side and two-side heat generation, dissipating 150 kW to 450 kW of heat with maximum junction temperatures of 150°C to 300°C.

✧ ✧ ✧ ✧ ✧

Introduction

All commercially available electric-drive vehicles, with the notable exception of the low-power Honda system, use liquid-cooled power electronics systems. All the heat from a vehicle, however, must ultimately be rejected to the air. For liquid-cooled systems, heat from the power electronics is transferred to a water-ethylene glycol coolant via a heat exchanger and then pumped to a separate, remote liquid-to-air radiator where the heat is rejected to the air. Air cooling has the potential to eliminate the intermediate liquid-cooling loop and transfer heat directly to the air.

Eliminating the intermediate liquid-cooling loop using direct air cooling of the power converter can reduce system complexity and cost by removing or reducing the pump, coolant lines, remote heat exchanger, remote heat exchanger fan, and coolant. To realize these gains, however, effective system-level design of the direct air-cooled system heat exchanger, fan, and ducting is needed. Decoupling the inverter/converter from the liquid cooling system also has the potential to provide increased flexibility in location. Honda took advantage of this benefit by placing its 12.4-kW power electronics system behind the rear seat of the vehicle cabin and integrating it closely with the battery thermal management system [1].

As power electronics semiconductor and electronic packaging technology advances, higher allowable junction temperatures will further expand the feasible designs and benefits of direct air-cooled power electronics. Currently, silicon insulated gate bipolar transistors have a maximum allowable junction temperature between 125°C and 150°C [2,3] that may be extended to 175°C in the future [3], while advanced semiconductor technologies such as silicon carbide (SiC) and gallium nitride allow operation above 200°C [4–6] and may also improve the inverter efficiency at lower temperatures [5].

The Honda system is a mass-produced, commercially available solution. It is low power, however, with a peak power delivery of 12.4 kW [1]. The electric Mini-E uses an air-cooled AC Propulsion drive system. This has a 50-kW continuous, 150-kW peak power, but does not meet DOE technical targets and the volume of production is low [7]. Toshiba Corporation is researching and developing a new power module design for forced-air cooling systems for a power converter [8]. ETH Zurich University has published a number of studies on this topic recently and is actively researching high-temperature, air-cooled power electronics for automotive and other applications. One of these papers found that, combined with a Peltier element, a high-temperature SiC automotive inverter could operate at a 120°C ambient [9]. Another reports the possibility of using extremely high-temperature SiC devices (234°C and higher) to create an air-cooled electric-drive vehicle inverter with a power density of 51 kW/L and operating at 120°C ambient [10]. For aggressive, high-flux cooling of electric-drive vehicle inverters, Aqwest is investigating circulating liquid metal flow loops to enable forced-air cooling [11].

Approach

Project

- Use a system-level approach that addresses the cooling technology, package mechanical design, balance-of-system, and vehicle application requirements
- Research each of these areas in depth and apply findings to develop effective system-level designs
- Develop experimental and analytical/numerical tools and processes that facilitate high-quality and rapid research results
- Investigate the effect high-temperature power semiconductor devices have on air-cooled inverter design
- Work closely with industry, university, and national laboratory partners to ensure relevant and viable solutions.

The objective of this project is to assess, develop, and apply air-cooling technology to improve power electronics thermal management design and influence industry's products, thereby enhancing the ability to meet DOE technical targets for weight, volume, cost, and reliability. This research effort seeks to develop the necessary heat transfer technology and system-level understanding to eliminate the intermediate liquid-cooling loop and transfer heat directly to the air. The relative merits of air-cooled, high-heat-flux automotive power electronics thermal management systems and the influence of high-temperature, wide bandgap semiconductors on this design space will be quantified, evaluated, and demonstrated under steady-state and transient conditions. See previous reports for more detail on the overall project objectives [12].

In FY14, an optimized heat exchanger was down selected after modeling efforts examined various geometric configurations. Baseline and optimized sub-modules were fabricated and tested to validate dissipation of the target heat load. A module-level heat exchanger that took into account the desired electrical topology was fabricated and characterized.

Experimental Methods

A baseline air-cooled heat exchanger consisting of an aluminum heat sink with equally spaced rectangular channels was proposed [13]. Devices would be mounted to both sides to use the channel wall fins more effectively. The design incorporated nine modules for a full inverter with a 30-kW continuous and 55-kW peak (for 18 seconds) electrical power output. This design did not meet targeted 12-kW/L power density and 12-kW/kg specific power requirements, proposed as 2015 targets by the U.S. DRIVE Electrical and Electronics Technical Team [14]. For this inverter size and number of devices, the total power loss to heat was conservatively estimated to be 2.7 kW (using device loss information and analytical equations) [12].

Through a parametric computational fluid dynamics study, the heat sink was optimized for weight and volume by varying

geometric parameters, including channel height, length and width, and device location. A constant heat flux was simulated for the devices, and the maximum allowable junction temperature for any device was set at 175°C. Two heat fluxes were investigated: one for an inverter with nine modules, and a higher flux for an inverter with six modules (lower weight and volume, but higher current and losses in each device). From this study, an optimized design was selected that met the specific power and power density targets [12].

Sub-module heat exchangers, which represent one-sixth of a full module, were prototyped for the baseline and optimized geometries from 6063 aluminum using wire electrical discharge machining (see Figure 1). A module-level heat exchanger was fabricated after sub-module testing and interaction with the electrical component layout. For mass manufacturing, final module-level heat exchangers could be manufactured using extrusion methods.

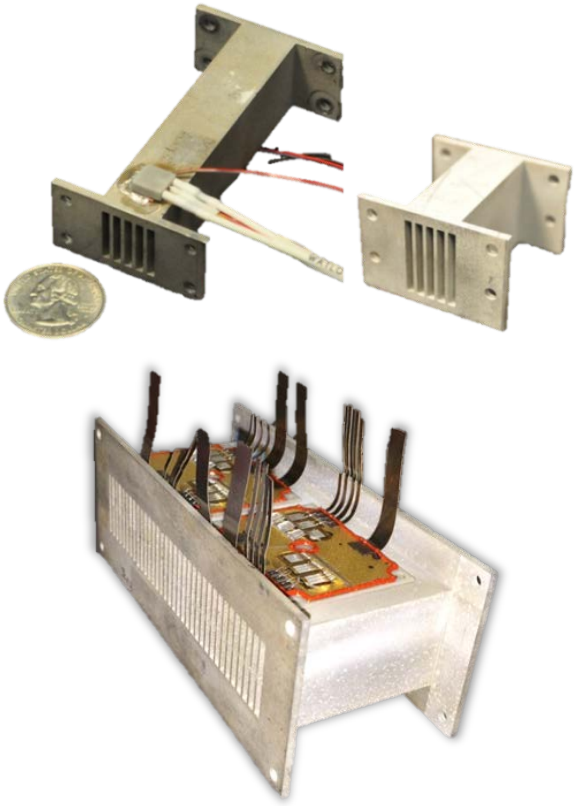

Figure 1. Baseline sub-module (top left), optimized (top right) sub-module, and module-level (bottom) heat exchangers fabricated from 6063 aluminum. Heaters are mounted on the top and bottom of the test section, one near the inlet edge and the other farther back. The flanges are for experimental convenience. The module-level heat exchanger shows electrical components mounted (tested by ORNL). Photo credit (bottom): Madhu Chinthavali, courtesy ORNL.

For the sub-module heat exchanger, channels for both baseline and optimized configurations were 2 mm wide with 1-mm-thick fin walls. The baseline channels were 15 mm tall and 74 mm long. The optimized channels were 21 mm tall and 40 mm long. The material thickness between the channels and the devices was 2.8 mm, calculated to nearly match the thermal resistance of a direct-bond-copper or direct-bond-aluminum substrate layer.

For the module-level heat exchanger, the channel and fin thicknesses were the same as the sub-module heat exchangers. The channels were 21 mm tall and 52.7 mm long. The material thickness between the channels and the devices was 4.0 mm to allow for electronic component attachment.

The test bench for this project (see Figure 2) used compressed air that was dried with a desiccant dryer to a dew point of -20°C or lower. The air was then passed through a 5-μm particulate filter and regulated at a pressure of 68 to 137 kPa. A mass flow controller provided the desired flow rates. A downstream laminar flow element was used to more accurately measure the flow rate and feedback to control the mass flow controller. The house air compressor was the limiting factor in maintaining the flow at adequate pressure throughout the experiment. Therefore, the maximum flow rate tested was 500 m^3/h for the module-level heat exchanger. The air passed through a plate heat exchanger for temperature control and entered the heat exchanger test section. The inlet temperature was set at 50°C, which is a conservative worst-case scenario for ambient air intake during vehicle operation.

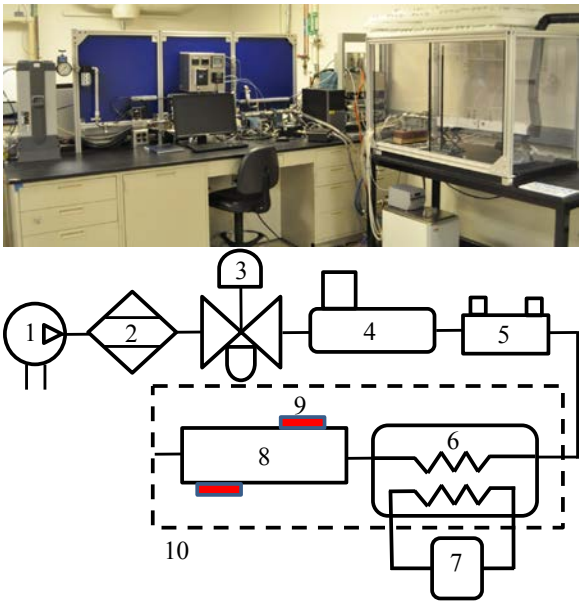

Figure 2. Air cooling test bench photo and schematic: (1) compressed air, (2) desiccant dryer, (3) filter/regulator, (4) mass flow controller, (5) laminar flow element, (6) plate heat exchanger, (7) temperature control bath, (8) fin test section, (9) ceramic resistance heaters, (10) isolation box.

Ceramic resistance heaters (8 mm × 8 mm) provided the heat load; power was adjusted to yield the desired junction temperature for each flow rate. A 0.5-mm-thick copper base plate with an embedded thermocouple was attached with thermal epoxy to the test section. Indium foil was placed between the copper base plate and the heater, topped with insulation, and held in place with a clamp (see Figure 3). The

test section was wrapped in insulation. For more details of the experimental setup, see Waye et al. [12]. A similar setup was used for the module-level heat exchanger, as shown in Figure 4.

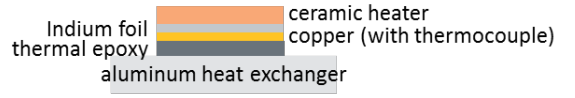

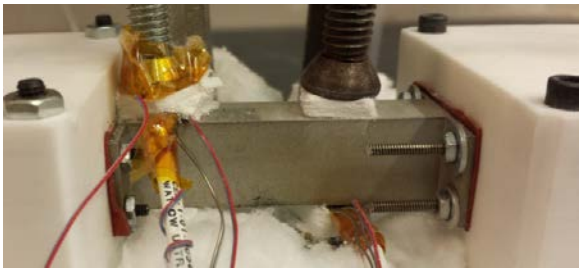

Figure 3. Heater stack-up and assembled sub-module (fin test section indicated by (8) and (9) in Figure 2).

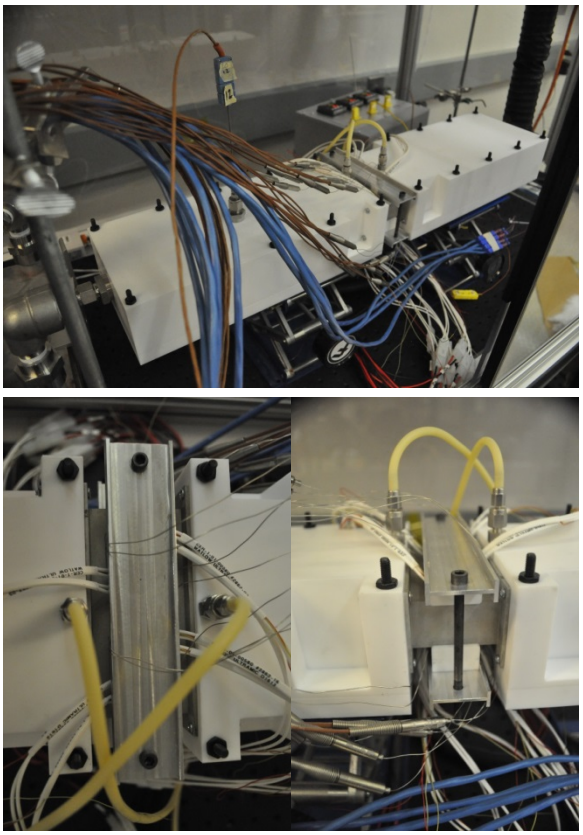

Figure 4. Module-level test setup (fin test section indicated by (8) and (9) in Figure 2). The top photo shows the inlet and outlet manifolds (white blocks) with the fin test section between them, shown in more detail in the bottom photos. The white wires are leads to heaters, clamped down with a small aluminum I-beam and rigid insulation. The yellow tubes are used for the pressure measurement.

Tests were conducted over a range of flow rates with a maximum junction temperature for any of the heaters. The power supplied to the heaters (dissipated as heat) and the pressure drop were measured for each flow rate. The heat dissipation and pressure drop results were extrapolated from the sub-module level to inverter scale; one module consisted of six sub-modules, and nine or six modules made up the entire inverter for the baseline and optimized configurations, respectively. To estimate the total inverter weight and volume, weights and volumes of the inverter components were combined with the heat exchanger assembly. The casing for each module was scaled for the heat exchanger geometry. The bus bars were assumed to be 0.088 kg per module. The capacitor was assumed to be 1.62 kg and 1.13 L. The gate driver and control board were assumed to be 0.42 kg and 0.88 L. Figure 5 shows the module-level heat exchanger and inverter assembly. An inverter casing was not included in the calculations.

The parasitic power of the system was of interest. Pressure drops across two production ducts (from other air intake systems) were combined to act as a surrogate inlet and exhaust ducting path for the air-cooled inverter system [12]. The total pressure drop of the system was calculated by using the flow rate through the heat exchanger.

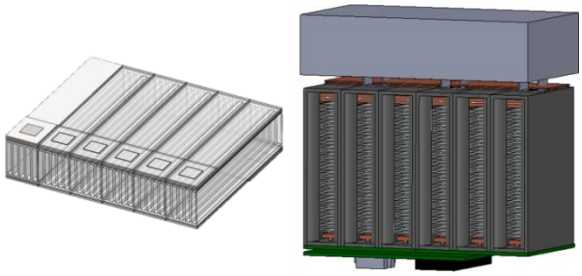

Figure 5. Schematic of module-level heat exchanger (left) with devices (six on top, six on bottom), and six-module inverter (right), including module casing, capacitor, bus bars, control board, and gate driver board. Computational fluid dynamics and experiments were conducted on the sub-module heat exchanger (opaque portion on far left of module-level heat exchanger).

Results

The heat dissipation for the baseline and optimized configurations is shown in Figure 6. Error bars represent 95% confidence levels. The target heat dissipation rate was 2.7 kW, which equates to an approximately 95% efficient inverter at peak power (55 kW).

Two production ducts for other applications were tested for pressure loss as a function of flow rate [12]. The ducting path would be designed for each vehicle platform and vary, so these ducts provide an estimate of the air intake and exhaust pressure losses. This pressure loss curve was combined with the pressure loss through the heat exchanger to provide an estimated system pressure drop, which is shown in subsequent plots and used in the calculation of the fluid power.

For the baseline configuration with nine modules, approximate air flow rates of 226, 100, and 70 m^3/h [132, 56,

41 ft³/min] for 150°C, 175°C, and 200°C maximum junction temperatures, respectively, met the heat dissipation rate target. The power density and specific power for the inverter components are estimated at 10.1 kW/L and 8.9 kW/kg, respectively. The fluid power (the product of flow rate and pressure drop, a parasitic load) to maintain a maximum junction temperature of 175°C was approximately 4 W (40 W for 150°C and 1.5 W for 200°C).

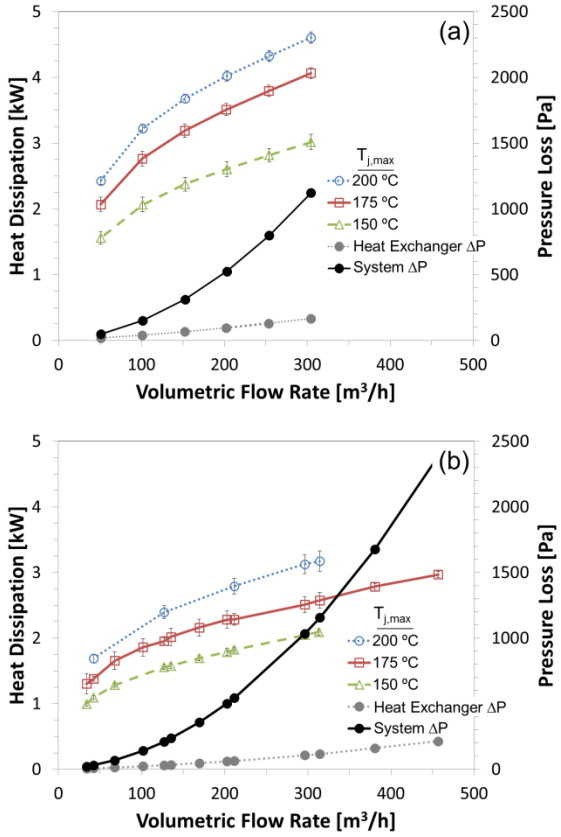

Figure 6. Heat dissipation curves and system pressure loss as a function of flow rate and maximum junction temperature for (a) baseline nine-module inverter*, and (b) optimized six-module inverter* configurations. The target heat dissipation is 2.7 kW. *Extrapolated to inverter level.

Reducing the number of modules reduces weight and volume, but also reduces the number of devices. To compensate and provide the same power, more current must run through the devices, which also increases heat dissipation. Using the optimized heat exchanger, 2.7 kW of heat was dissipated at approximate airflow rates of 384, 230, 79, 44, and 20 m³/h [225, 136, 47, 26, and 12 ft³/min] for maximum junction temperatures of 175°C, 200°C, 225°C, 250°C, 275°C, and 300°C, respectively. At 150°C, no flow rate tested could dissipate 2.7 kW of heat using the heat exchanger with the optimized design and six-module configuration. The power density and specific power of the inverter components rose to 14.5 kW/L and 13.2 kW/kg. The tradeoff of a more compact design is increased fluid power: approximately 183 W, 45 W, 3.5 W, and 0.5 W for the 175°C, 200°C, 250°C, and 275°C maximum junction temperature, respectively. As previously stated, at 150°C, no flow rate dissipated the target heat load. At 300°C maximum junction temperature, the lowest flow rate dissipated more heat than the target load.

For each case, a fan must be sized to provide the fluid power, and the fan efficiency must be considered. A typical air conditioning system blower or compressor fan uses up to around 150 W at peak demand.

The outlet temperature decreases with increased flow rate, as seen in Figure 7 for the optimized heat exchanger. The outlet temperatures for the optimized heat exchanger were also lower when compared to the baseline configuration for any given junction temperature. When the heat exchanger dissipated 2.7 kW of heat at 175°C maximum junction temperature, the outlet temperature for the baseline configuration was approximately 100°C. The optimized configuration outlet temperature was approximately 68°C.

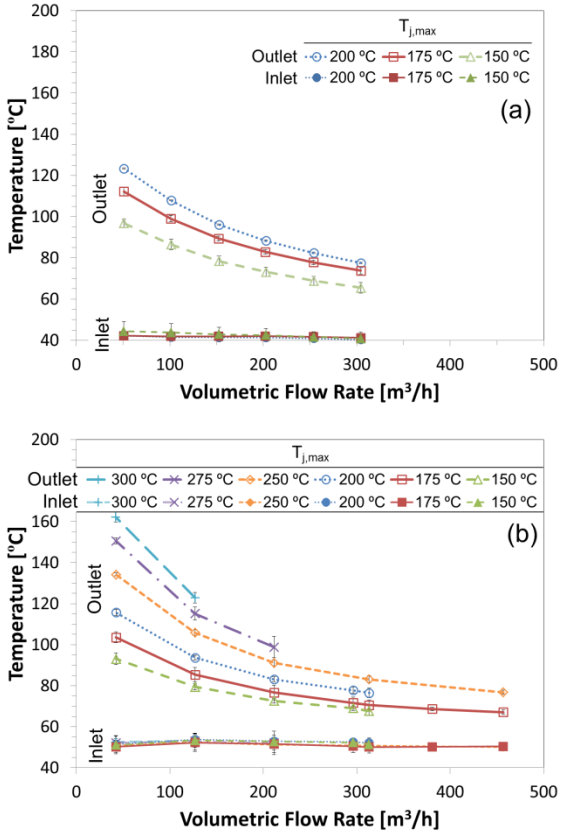

Figure 7. Inlet and outlet air temperatures as a function of flow rate and maximum junction temperature for the (a) baseline and (b) optimized sub-module heat exchanger

For the baseline sub-module heat exchanger tests, the inlet temperature was approximately 45°C. For the optimized sub-module experiments, the inlet temperature was closer to 50°C. The effect of the inlet temperature was examined, as shown in Figure 8. For every 5°C increase in inlet temperature, the heat dissipation decreased by about 3% in the range tested.

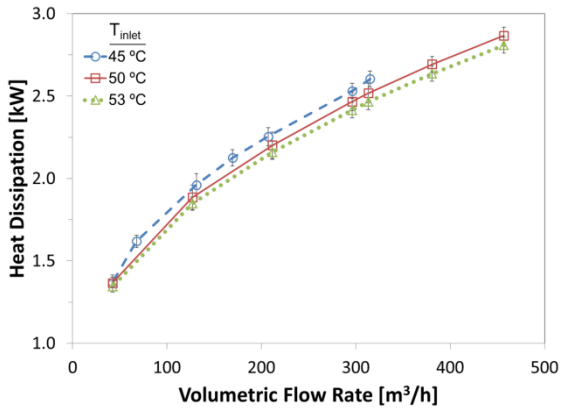

Figure 8. Inlet air temperature effect on heat dissipation for $T_{j,max}$ = 175°C

The design of the heat exchanger was iterated upon to meet electrical component layouts in collaboration with ORNL. Therefore, the design tested at the module level has lower thermal performance than the optimized geometry, but certain constraints had to be met to mount the electrical hardware. The layout tested is shown in Figure 9 (and the bottom picture in Figure 1), where there are four groups of transistor/diode device sets. In order to generate heat, two 8mm by 8mm ceramic resistance heaters were attached via the same method as previously addressed to each side of a module-level heat exchanger.

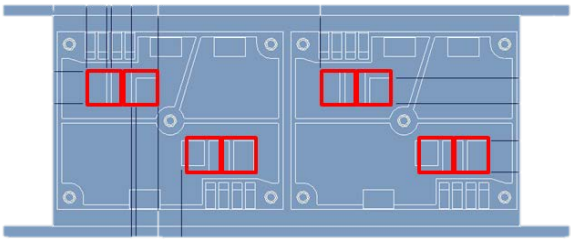

Figure 9. Location of ceramic resistance heaters overlaid on electrical design layout

The heat dissipation at maximum junction temperatures from 150°C to 300°C is shown in Figure 10. The results are presented as a characterization of the single module heat exchanger. Thus, the results have not been extrapolated to a full inverter (six or nine modules). The module was initially designed to produce 10 kW of electrical power, but further design and analysis indicate that more power may be produced, which would improve weight and volume metrics. The pressure losses for the heat exchanger and for an extrapolated system (ducting pressure loss added) are shown on the same plot, using the right-hand axis.

For most tests, all sixteen heaters (eight on each side) provided the heat load. For a few experiments, heaters on only one side were turned on. These are designated as "1-side" in the plot under the maximum junction temperature at which they were run. All error bars represent 95% confidence levels.

The heat exchanger dissipates more heat with higher maximum junction temperatures, mostly due to the fact that there is a higher temperature difference, which drives the heat transfer. The curves are relatively flat, indicating that an increased flow rate is creating diminishing benefits of heat dissipation. The heat dissipated when the heaters on only one side are on is about 90% of the heat dissipated with both sides turned on. Therefore, the heat exchanger can be thought of as nearly single-sided for all devices, where the fins are being shared by all heat sources.

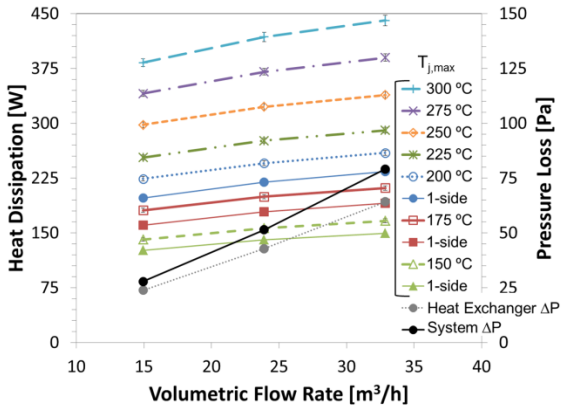

Figure 10. Heat dissipation curves and system pressure loss as a function of flow rate and maximum junction temperature for the module-level heat exchanger (not extrapolated to inverter level)

The inlet and outlet temperatures at the different maximum junction temperatures are shown in Figure 11. The temperatures are relatively low. Under-hood temperatures often rise to 140°C, so the exhaust heat from the inverter through the heat exchanger could be reasonably released under-hood or at another external location.

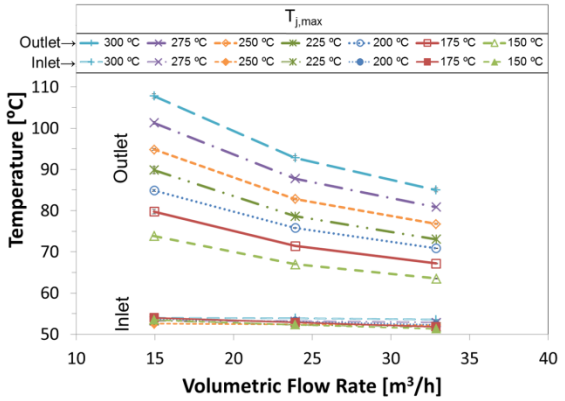

Figure 11. Inlet and outlet air temperatures as a function of flow rate and maximum junction temperature for the module-level heat exchanger

The maximum temperature of the thin copper plate epoxied to the surface was set to be the maximum junction temperature being tested. All other temperatures were lower, depending on the local cooling effectiveness of the heat exchanger. The heater temperatures were slightly higher to produce the heat flux necessary to maintain this temperature.

The heat source temperatures were plotted to examine the distribution of temperatures on the heat exchanger (Figure 12). The low, medium, and high flow rates tested are shown for three maximum junction temperatures (150°C, 175°C, and 200°C). In the figure, the air would flow into the page. A front view of the heat exchanger is accompanied by a top and bottom view for each flow rate and maximum junction temperature.

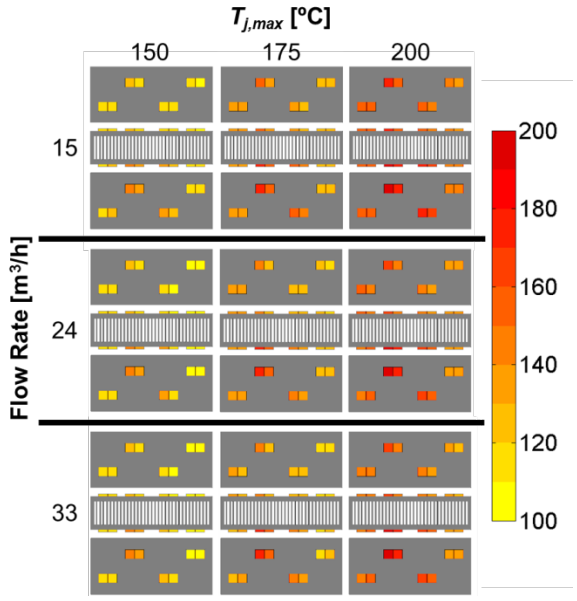

Figure 12. Temperature map for heat sources for three flow rates and maximum junction temperatures of 150°C, 175°C, and 200°C

Several observations can be made from the thermal mapping of the heat sources. The temperature distribution is quite sensitive to the flow through the heat exchanger. The local heat transfer was sensitive to the air flow distribution, creating non-isothermal conditions and temperature distributions. During setup of the test section, there was a noticeable mal-distribution of air through the inlet manifold. A baffle and screen were put in place to create a pressure drop and to make the flow more uniform. The uniformity of the flow rate through the heat exchanger was measured to be above 90%. The areas that had slightly lower flow were the same locations in the thermal map that had the highest temperatures. Thus, those areas controlled the location of the maximum junction temperature. The temperatures scaled proportionally to the maximum junction temperature, as shown in Figure 13 (high flow rate for all the maximum junction temperatures)

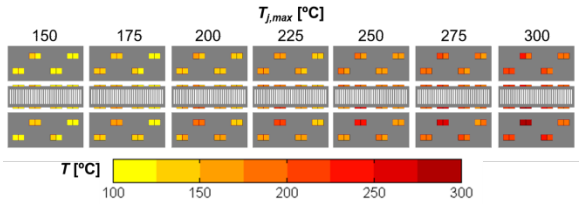

Figure 13. Temperature map of heat sources at high flow rate (33 m³/h)

Conclusions

An air-cooled heat exchanger for power electronics inverter thermal management provides a potential technology for low cost, simple-to-manufacture option for high temperature devices. It would potentially eliminate the liquid-to-air coolant loop typically used in automotive applications. It would also provide potential solutions to cooling components with lower temperature limits (e.g., 85°C capacitor) while the desired liquid cooling temperatures are increasing.

In the current work, the thermal performance for baseline and optimized sub-modules was characterized. A module-level heat exchanger was characterized, and thermal performance metrics were presented. The parasitic power of the systems is projected to be in line with other vehicle components, such as an air conditioning fan or condenser, which was deemed acceptable.

Higher junction temperatures provide opportunities for increased heat transfer and greater feasibility of an air-cooled heat exchanger system. Heat dissipation was measured for up to 300°C maximum junction temperatures. Packaging remains a challenge for these elevated temperatures, and thermal interface materials and reliability concerns need to be addressed to fully take advantage of higher device temperatures.

Reducing the number of modules (with a penalty of increased heat generation from increased current and increased parasitic power) is beneficial for weight and volume considerations. Full inverter components (including housing) need to be considered for weight and volume targets. Further optimization of the heat exchanger within the thermal and electrical constraints could further reduce weight and volume. More advanced heat exchanger designs may improve heat transfer efficiency with tradeoffs in manufacturability and cost. This requires co-design of the thermal and electrical systems. Understanding the complete inverter system, including ducting pathways, inverter location, and fan requirements is important when comparing to currently used systems.

FY 2014 Publications/Presentations

1. Waye, S. “High Temperature Air-Cooled Power Electronics Thermal Design.” Presentation, DOE Annual Merit Review; June 18, 2014, Washington D.C.

2. Waye, S. "High Temperature Air-Cooled Power Electronics Thermal Design." Presentation, EETT; August 27, 2014, Southfield, MI.
3. Waye, S.; Musselman, M.; King, C. "Air Cooling for High Temperature Power Electronics." Presentation, 2014 SAE Thermal Management Systems Symposium; September 23, 2014, Lakewood, CO.
4. Waye, S.; Lustbader, J.; Musselman, M.; King, C. "Air-Cooled Heat Exchanger for High-Temperature Power Electronics." 47th Symposium on Microelectronics: IMAPS 2014 – International Microelectronics Assembly and Packaging Society 2014, Oct 15, 2014, San Diego, CA.

Acknowledgments

The author would like to acknowledge the support provided by Susan Rogers and Steven Boyd, Technology Development Managers for Electric Drive Technologies, Vehicle Technologies Office, U.S. Department of Energy Office of Energy Efficiency and Renewable Energy. The significant contributions of Matt Musselman, Charlie King, and Kevin Bennion (NREL) to the project are acknowledged. Collaboration with Madhu Chinthavali from ORNL has been important in balancing the electrical and thermal design and constraints. The author would also like to acknowledge SAPA Extrusions USA for providing aluminum fin block prototypes.

References

1. Staunton, R.H., Burress, T.A., Marlino, L.D. *Evaluation of 2005 Honda Accord Hybrid Drive System*. ORNL/TM-2006/535. Oak Ridge, TN: Oak Ridge National Laboratory, September 2006.
2. *Semikron Application Manual* 1998. Section 3.1. Accessed on July 7th, 2011.
3. Matsumoto, S. "Advancement of Hybrid Vehicle Technology." *European Conference on Power Electronics and Applications,* Dresden, Germany, September 2005.
4. Uesugi, T., Kachi, T. "GaN Power Switching Devices for Automotive Applications." CSMan Tech Conference, Tampa, Florida, May 2009.
5. Renken, F., Knorr, R. "High Temperature Electronics for Future Hybrid Powertrain Application," *European Conference on Power Electronics and Applications*. Dresden, Germany, September 2005.
6. Funaki, T., Balda, J., Junghans, J., Kashyap, A., Mantooth, H., Barlow, F., Kimoto, T., Hikihara, T., 2007, "Power conversion with SiC devices at extremely high ambient temperatures," IEEE Transactions on Power Electronics, 22- 4, pp. 1321–1329.
7. Chow, Y. (media contact). "AC Propulsion Partners with BMW to Build 500 Electric Vehicles." Press release. 2008. http://www.acpropulsion.com/pressreleases/11.20.2008%20BMW%20Press%20Release.pdf . Accessed July 6th, 2011.
8. Kodani, K., Tsukinari, T., Matsumoto, T., "New Power Module Concept by Forced-Air Cooling System for Power Converter." *IEEE 2010 International Power Electronics Conference*, Sapporo, Japan, July 2010.
9. Bortis, D., Wrzecionko, B., Kolar, J.W. "A 120°C Ambient Temperature Forced Air-Cooled Normally-Off SiC JFET Automotive Inverter System." *IEEE 26th Annual Applied Power Electronics Conference and Exposition (APEC)*, Fort Worth, TX, March 2011.
10. Wrzecionko, B., Biela, J, and Kolar J. "SiC Power Semiconductors in HEVs: Influence of Junction Temperature on Power Density, Chip Utilization and Efficiency." *IEEE 35th Annual Industrial Electronics Conference,* Porto, Portugal, November 2009.
11. Vetrovec, J. "High-Performance Heat Sink for Interfacing Hybrid Electric Vehicles Inverters to Engine Coolant Loop." *SAE World Congress.* Paper# T11PFL-0459, Detroit, MI, April 2011.
12. Waye, S., Narumanchi, S., Lustbader, J., Bennion, K., Smith, C. "Air-Cooling Technology for Power Electronics Thermal Management." FY2013 EERE Vehicle Technologies Office Advanced Power Electronics and Electric Motors Annual Report, April 2014.
13. Chinthavali, M. "Gas Cooled Traction Drive Inverter," U.S. Patent No. 8,553,414 B2, issued October 8, 2013.
14. "Electrical and Electronics Technical Team Roadmap." U.S. DRIVE. http://www1.eere.energy.gov/vehiclesandfuels/pdfs/program/eett_roadmap_june2013.pdf, June 2013.